

## Macroporous Polystyrene Resins as Adsorbents for the Removal of Tetracycline Antibiotics from an Aquatic Environment

Yanhong Chao,<sup>1</sup> Wenshuai Zhu,<sup>1</sup> Bin Yan,<sup>1</sup> Yaobao Lin,<sup>1</sup> Suhang Xun,<sup>1</sup> Haiyan Ji,<sup>1</sup> Xiangyang Wu,<sup>1</sup> Huaming Li,<sup>1</sup> Changri Han<sup>2</sup>

<sup>1</sup>School of Pharmacy, School of the Environment, School of Chemistry and Chemical Engineering, Jiangsu University, Zhenjiang 212013, People's Republic of China

<sup>2</sup>Key Laboratory of Tropical Medicinal Plant Chemistry (Ministry of Education), Hainan Normal University, Haikou 571158, People's Republic of China

Correspondence to: W. S. Zhu (E-mail: zhuws@ujs.edu.cn) and X. Y. Wu (E-mail: wuxy@ujs.edu.cn)

**ABSTRACT:** Six macroporous polystyrene resins (strong-acid resins D001, D061, D072, and NKC-9, strong-base resin D201, and alkaline resin D370) were selected as adsorbents for removing tetracycline (TC) and doxycycline hydrochloride (DC) from aqueous solutions. The solution pH and ionic strength had significant effects on the sorption of TC and DC. The basic resins D201 and D370 exhibited strong sorption capabilities (70.08–105.60 mg/g) at pH 4–9, but strong-acid resins showed good sorption abilities only under acidic conditions of pH 2–3 (83.30–95.78 mg/g). The inhibitory effect of the ionic strength was much weaker for D370 than for D201. The adsorption ratio of TC and DC on D201 and D370 were all above 90% when the amount of adsorbent exceeded 50 mg. By performing kinetic experiments, we determined that the pseudo-second-order model fit the data best for DC sorption on the six resins and TC sorption on D201 and D370, but the pseudo-first-order model fit the data of TC sorption on the four strong-acid resins better at pH 7.0. Intraparticle diffusion was not the only rate-controlling step, and an initial external mass transfer or chemical reaction might have existed in the sorption process. The Langmuir equation was the best isotherm equation to describe the sorption with a monolayer sorption maximum larger than 98.04 mg/g under all temperatures. Thermodynamic studies showed that the sorption of TC and DC on the resins was thermodynamically feasible and spontaneous. © 2014 Wiley Periodicals, Inc. *J. Appl. Polym. Sci.* **2014**, *131*, 40561.

**KEYWORDS:** adsorption; kinetics; resins

Received 6 November 2013; accepted 2 February 2014

DOI: 10.1002/app.40561

### INTRODUCTION

Antibiotics have been used extensively to control infection in humans and livestock, and their global market consumption increases steadily every year. However, most antibiotics are poorly absorbed and are continually excreted into the environment as active metabolites. The gradual increase of antibiotics in soils, surface water, and groundwater pose a serious threat to human health.<sup>1</sup> Bacteria have been observed to develop drug-resistance genes during long-term contact with antibiotics.<sup>2</sup> More and more infections may no longer be treatable with known antibiotics. Therefore, the removal of such organic contaminants from water has created great public concern.

Up to this point, a great number of chemical and physical methodologies for the removal of pharmaceutical antibiotics has been developed, for instance, the advanced oxidation tech-

nique,<sup>3</sup> an electrochemistry process,<sup>4</sup> membrane filtration,<sup>5</sup> and the adsorption method.<sup>6</sup> The nondestructive adsorption method is considered to be one of the most effective measures with its low energy consumption for the treatment of contaminants.<sup>7</sup> Recent studies on antibiotic adsorption removal have focused on the use of natural or engineered adsorbents, such as soils,<sup>8</sup> clay minerals (e.g., montmorillonite,<sup>9</sup> zeolite,<sup>10</sup> palygorskite,<sup>11</sup> struvite<sup>12</sup>), carbonaceous adsorbents (activated carbons,<sup>13,14</sup> carbon nanotubes,<sup>15–18</sup> graphene oxide,<sup>19</sup> biomass ashes<sup>20</sup>), mesoporous siliceous materials,<sup>21</sup> and polymer resins.<sup>22</sup>

Among these adsorbents, polymer resins are regarded as a good choice because of their striking characteristics, including low cost, high porosity, large surface area, and great adsorption capacity.<sup>23</sup> The most attractive feature is that it can be regenerated more easily than other materials. So far, some kinds of resins had been used successfully to remove common antibiotics

Additional Supporting Information may be found in the online version of this article.

© 2014 Wiley Periodicals, Inc.

from aquatic solutions, such as the hypercrosslinked resins, aminated polystyrene resins, macroporous resins, microporous resins, and magnetic resins.<sup>24–29</sup> Butler et al.<sup>30</sup> chose a series of neutral and anion-exchange polymers to remove nalidixic acid. Their results demonstrate that the pH and adsorbent structure were the most important factors determining the antibiotic–adsorbent interactions, and they eventually affected the adsorption capacity. However, information on the adsorption behavior and mechanisms of antibiotics to resins is still relative lacking.

The main objective of this study was to systematically investigate the mechanism and predominant factors controlling antibiotic adsorption onto ion-exchange resins in aqueous solution. Six economical macroporous polystyrene resins, the strong-acid cation-exchange resins D001, D061, D072, and NKC-9; the strong-base anion-exchange resin D201; and the alkaline anion-exchange resin D370, were selected as adsorbents. Tetracycline (TC) and doxycycline hydrochloride (DC), two of the most commonly used tetracycline antibiotics (TCs) were chosen as model drugs. The adsorption kinetics, isotherms, thermodynamics, and effects of solution pH, adsorbent dose, and ion strength were evaluated in batch adsorption experiments. These results will provide a theoretical foundation for further applications of these resins in the removal of antibiotics from wastewater.

## EXPERIMENTAL

### Materials

TC and DC (99% pure) were obtained from Sigma-Aldrich Chemical Co. and were used as received. All of the resins in this study, including D001, D061, D072, NKC-9, D201, and D370, were purchased from Nankai University Chemical Factory. The structures and some physicochemical properties of the two antibiotics and six resins are summarized in the Supporting Information (Table S1). The water used in the study was purified by distillation. HCl, NaOH, and ethanol were supplied by Sino-pharm Chemical Reagent Co., Ltd. (analytical-reagent grade).

### Pretreatment of the Resins

Before use, all of the resins were washed with distilled water, a 1.0 mol/L HCl solution, a 1.0 mol/L NaOH solution, and ethanol to remove impurities in the following steps. The resins were first washed by distilled water, then rinsed with 1.0 mol/L NaOH, and finally washed by distilled water to pH 6–7. Next, the resins were rinsed with 1.0 mol/L HCl and again flushed with distilled water to reach a neutral pH. Finally, the resins were stirred with ethanol for 4 h and then vacuum-desiccated at 325 K overnight.

### Adsorption Experiments

Adsorption experiments (in darkness to prevent photodegradation) were performed with a batch equilibration procedure with 100-mL conical flasks in a thermostatic shaker bath at a preset temperature of 298 K and a shaking speed of 130 rpm. An amount of 50 mg of adsorbent was introduced into the flasks and then mixed with 50 mL of a 100 mg/L TC or DC solution. The solution pH was adjusted with 0.01 mol/L HCl or NaOH. If necessary, the ionic strength of the solution was adjusted by the dissolution of different amounts of NaCl solid before the addition of the resins. At different reaction times, 5 mL of

supernatant was aspirated and analyzed immediately. After quantification, which took around 30 s, the supernatant was reintroduced into the flasks. This procedure (separation, quantification, and reintroduction) was repeated over several hours to achieve complete adsorption or to gather enough data points. Adsorption isotherm studies were carried out with initial adsorbate concentrations ( $C_0$ ) of 20, 40, 60, 80, and 100 mg/L. The experimental temperatures were controlled at 288, 298, 308, and 318 K, respectively. The concentration of the antibiotics was determined by UV spectroscopy (UV2401, PC) at 358 nm (TC) and 345 nm (DC). Linear calibration curves (absorbance vs concentration) were used to determine the concentrations of the antibiotics. The adsorption data were collected in duplicate for the adsorption kinetics and isotherms experiments and in triplicate for all of the other experiments. The adsorption capacity [ $q_e$  (mg/g)] was calculated with eq. (1). The adsorption ratio (Ads.%) was calculated with eq. (2):

$$q_e = V(C_0 - C_e) / m \quad (1)$$

$$\text{Ads. \%} = (C_0 - C_e) / C_0 \times 100 \quad (2)$$

where  $C_e$  is the residual concentration at equilibrium (mg/L),  $V$  is the volume of solution (L), and  $m$  is the mass of dry resin (g).

### Adsorption Kinetics and Isotherm Models

The adsorption kinetics and adsorption isotherms are of crucial importance in the design of adsorption systems. In this study, three kinetic models, the pseudo-first-order model, pseudo-second-order model, and intraparticle diffusion model, were used to analyze the kinetics data of TC and DC adsorption on the six adsorbents. Three isotherm models, the Langmuir, Freundlich, and Tempkin models, were applied to fit the equilibrium data of TC and DC adsorption on the three selected resins at perfect pH conditions. The linear forms of these models and some key parameters are listed in the Supporting Information (Table S2).

## RESULTS AND DISCUSSION

### Adsorption Kinetics

Figure 1 presents the adsorption kinetics of TC and DC on the six resins at pH 7.0. We found that the strong-base resin D201 and alkaline resin D370 had much higher adsorption capacities ( $q_e = 96.6$ – $105.6$  mg/g) than the strong-acid resins D001, D061, D072, and NKC-9 ( $q_e = 24.2$ – $42.6$  mg/g) for both TC and DC at pH 7.0. The shapes of the kinetics curves for D201 and D370 were similar and exhibited a fast initial adsorption with an adsorption capacity of 90% accomplished within the first 24 h. Then, adsorption was followed by a slow diffusion process, and equilibrium was reached at about 96 h.

To evaluate the kinetic adsorption mechanism, the pseudo-first-order and pseudo-second-order models were applied to analyze the experimental data. The kinetic parameters are summarized in Table I. As shown in Figure 1 and Table I, the pseudo-second-order model provided the best match for the data of DC sorption onto the six resins and TC sorption onto D201 and D370 according to the good correlation coefficient ( $R^2 > 0.9953$ ), which indicated that these sorption processes were controlled by chemisorption under studied conditions.<sup>31</sup> However, the pseudo-first-order model fit the data of TC

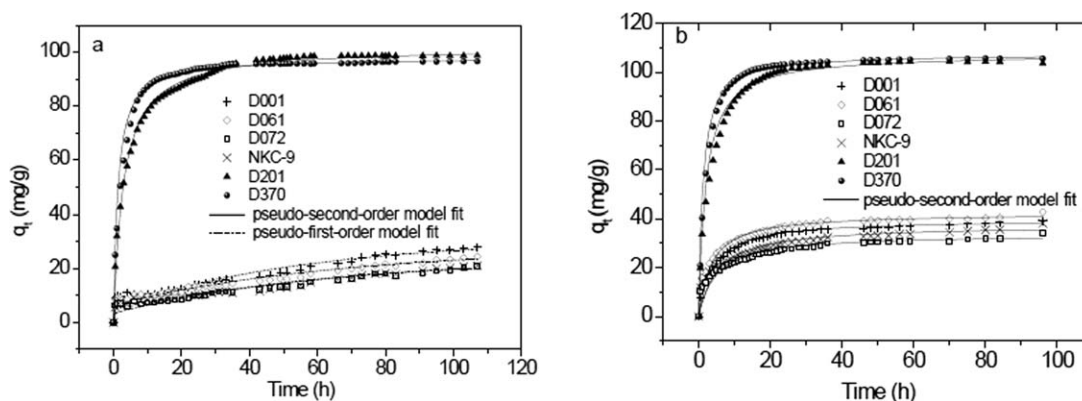


**Figure 1.** Adsorption kinetics of (a) TC and (b) DC for the six resins according to pseudo-first-order and pseudo-second-order models.

sorption onto the other four strong-acid resins better with a higher  $R^2$ ; this suggested that the physisorption processes might have dominated the sorption of TC on these cation-exchange resins at pH 7.0. Moreover, the agreement of the equilibrium sorption capacity between the calculated data and the experimental data ( $q_{e,exp}$ ) also confirmed the previous results.

To predict the rate-controlling steps affecting the kinetics, the intraparticle diffusion model was tested. The plots of the adsorption capacity at time  $t$  ( $q_t$ ) against the square root of time ( $t^{1/2}$ ) for this model are presented in supporting information (Fig. S1). The plots exhibited multilinearity, and this showed that two or more steps might have influenced the sorption process. The first sharper portion was attributed to the external mass transfer or external film resistance. The second portion described the gradual sorption stage, where the intraparticle diffusion was rate-limiting. For resins D201 and D370, the third portion, which was the final equilibrium stage, existed, where intraparticle diffusion started to slow down because of

the smaller pores or the enhanced electrostatic repulsion, and the extremely low adsorbate concentrations left in the solutions might also have been one reason for this. The sorption rate ( $k_{di}$ ) and  $I_i$  values of the corresponding stages are listed in the Supporting Information (Table 4).  $I_i$  reflects the extent of the boundary layer thickness. The  $k_{di}$  values decreased, and the  $I_i$  values, increased with time during the sorption process. Moreover, the linear sections of all of the curves did not pass through the origin, and this demonstrated that intraparticle diffusion was not the only rate-controlling step, and some other mechanisms, such as initial external mass transfer or chemical reaction, might have been involved.<sup>32</sup>

### Effect of pH

The effect of pH on the sorption of TC and DC onto the six resins was studied, and the results are depicted in Figure 2. It was reported that the solution pH played an important role in the TC sorption onto polymer resins.<sup>27,33</sup> Similarly, the sorption

**Table I.** Pseudo-First-Order and Pseudo-Second-Order Kinetic Parameters for the Adsorption of TC and DC onto the Six Resins

Adsorbate	Resin	$q_{e,exp}$ (mg/g)	Pseudo-first-order model			Pseudo-second-order model				
			$q_{e,1}$ (mg/g)	$k_1$ (h <sup>-1</sup> )	$R^2$	$q_{e,2}$ (mg/g)	$k_2$ (g·mg <sup>-1</sup> ·h <sup>-1</sup> )	$h$ (mg·g <sup>-1</sup> ·h <sup>-1</sup> )	$t_{1/2}$ (h)	$R^2$
TC	D201	98.776	51.998	0.081	0.9540	102.041	0.003	35.336	2.888	0.9997
	D370	96.633	16.382	0.055	0.8627	98.039	0.008	78.125	1.255	0.9999
	D001	31.361	25.718	0.017	0.9656	33.898	0.001	1.207	28.085	0.9346
	D061	28.096	21.568	0.015	0.9701	29.240	0.001	1.140	25.652	0.9383
	D072	24.218	20.841	0.016	0.9679	25.575	0.001	0.803	31.847	0.9171
	NKC-9	25.307	20.446	0.013	0.9541	26.178	0.001	0.833	31.419	0.8991
DC	D201	104.280	42.760	0.093	0.9432	107.527	0.005	53.476	2.011	0.9997
	D370	105.600	21.430	0.071	0.9104	107.527	0.008	90.909	1.183	0.9999
	D001	39.080	16.305	0.039	0.9207	39.841	0.007	10.331	3.857	0.9993
	D061	42.640	15.501	0.029	0.8459	42.373	0.007	12.270	3.453	0.9988
	D072	34.120	15.336	0.027	0.9150	33.784	0.006	6.916	4.885	0.9968
	NKC-9	38.200	17.807	0.025	0.9327	37.453	0.005	7.153	5.236	0.9953

$k_1$ : the rate constant of the pseudo-first-order.

$k_2$ : the rate constant of the pseudo-second-order.

$h$ : the initial sorption rate.

$t_{1/2}$ : the half-equilibrium time.

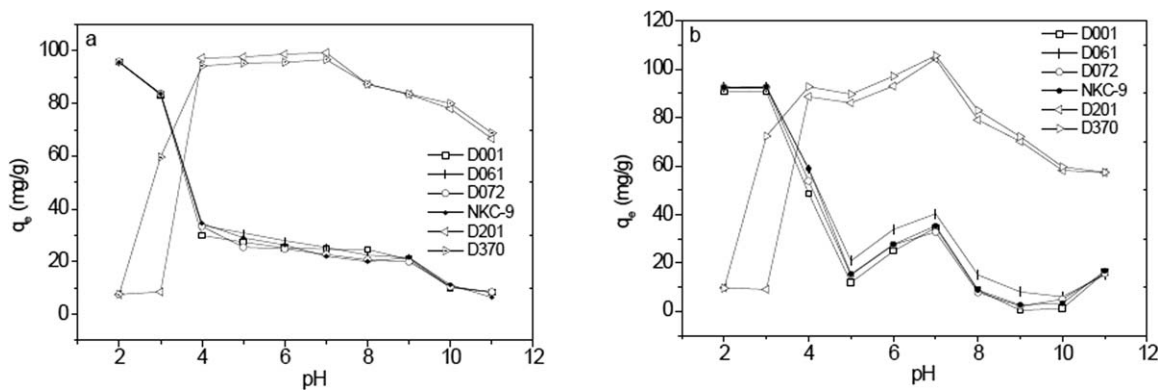


Figure 2. Effect of pH on the adsorption of (a) TC and (b) DC onto the six resins.

of TC and DC onto the six ion-exchange resins also exhibited strong pH dependence between pH values of 2 and 11. As shown in Figure 2, we found that the strong-base resin D201 and alkaline resin D370 exhibited a strong sorption ability under pHs 4–9 and 3–9, respectively, whereas the four strong-acid resins showed good sorption capabilities at pH 2–3.

For TC, as shown in Figure 2(a), the sorption capacity onto D201 and D370 increased obviously with increasing pH values from 2 to 4 and reflected the strong sorption capacity in the pH range 4–7 but gradually decreased when pH value was greater than 7. However, for the strong-acid resins D001, D061, D072, and NKC-9, the sorption capacity of TC exhibited a sharply decreasing trend when the pH changed from 2 to 4 and with a slight change at pH 4–9 and then decreased obviously again when pH was above 9. These results of the pH indicated that the optimized condition for TC removal was pH 4–7 for D201 and D370 and a low pH of less than 4 for the four strong-acid resins. Meanwhile, as shown in Figure 2(b), DC sorption was also dependent on pH. For the basic resins D201 and D370, the sorption capacity of DC increased when the solution pH rose from 2 to 7 and decreased quickly when the pH values was above 7. This indicated that the strongest sorption capability was found under conditions of pH 7 for DC. How-

ever, for the four strong-acid resins, the acidic conditions at  $\text{pH} < 4$  were the best.

The observed pH effects on the sorption of TC and DC on the six resins were related to the aromatic rings and the functional groups present on the structures of the adsorbates and adsorbents; from this, we could deduce to the supposed mechanisms of the hydrophobic effect, electrostatic interaction, and  $\pi$ - $\pi$  electron donor-acceptor (EDA) interaction. As shown in Table S1 in the Supporting Information, both TC and DC had three  $\text{pK}_a$  values, and this caused them to exist as cationic, neutral (including zwitterionic), and anionic species, respectively, under different pH conditions. At pH values between 4 and 7, the forms existed, with the neutral form being dominant.<sup>27</sup> The adsorption capability increased with increasing zwitterionic form and enhanced to the highest values for D201 and D370 at pH 7 (Figure 2). This demonstrated that the contribution of neutral form to adsorption affinities on the resins was greater than that of the ionic forms. The deprotonated species (anionic or cationic form) of TC and DC were apparently much less hydrophobic compared to their neutral counterparts. The polystyrene-divinylbenzene matrices of the resins provided hydrophobic sites that could interact with the TC and DC molecules by hydrophobic effects. So, the hydrophobic effect played an important role in the sorption process. On the

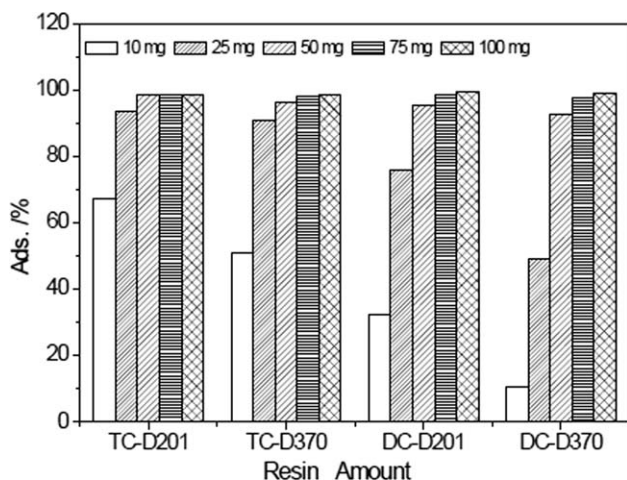


Figure 3. Effect of the amounts of resins D201 and D370 on the adsorption of TC and DC.

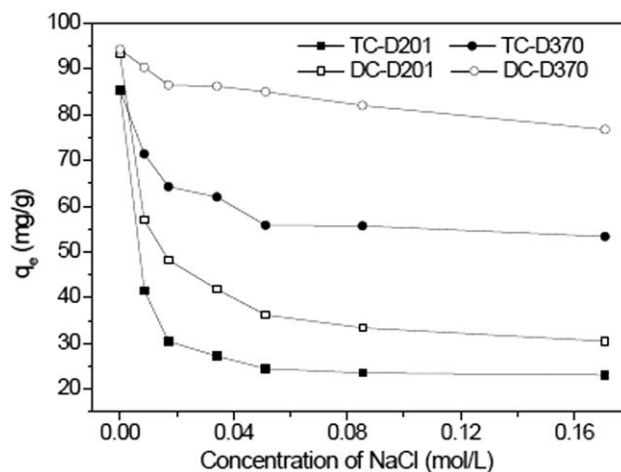


Figure 4. Effect of the ionic strength on the adsorption of TC and DC onto resins D201 and D370.



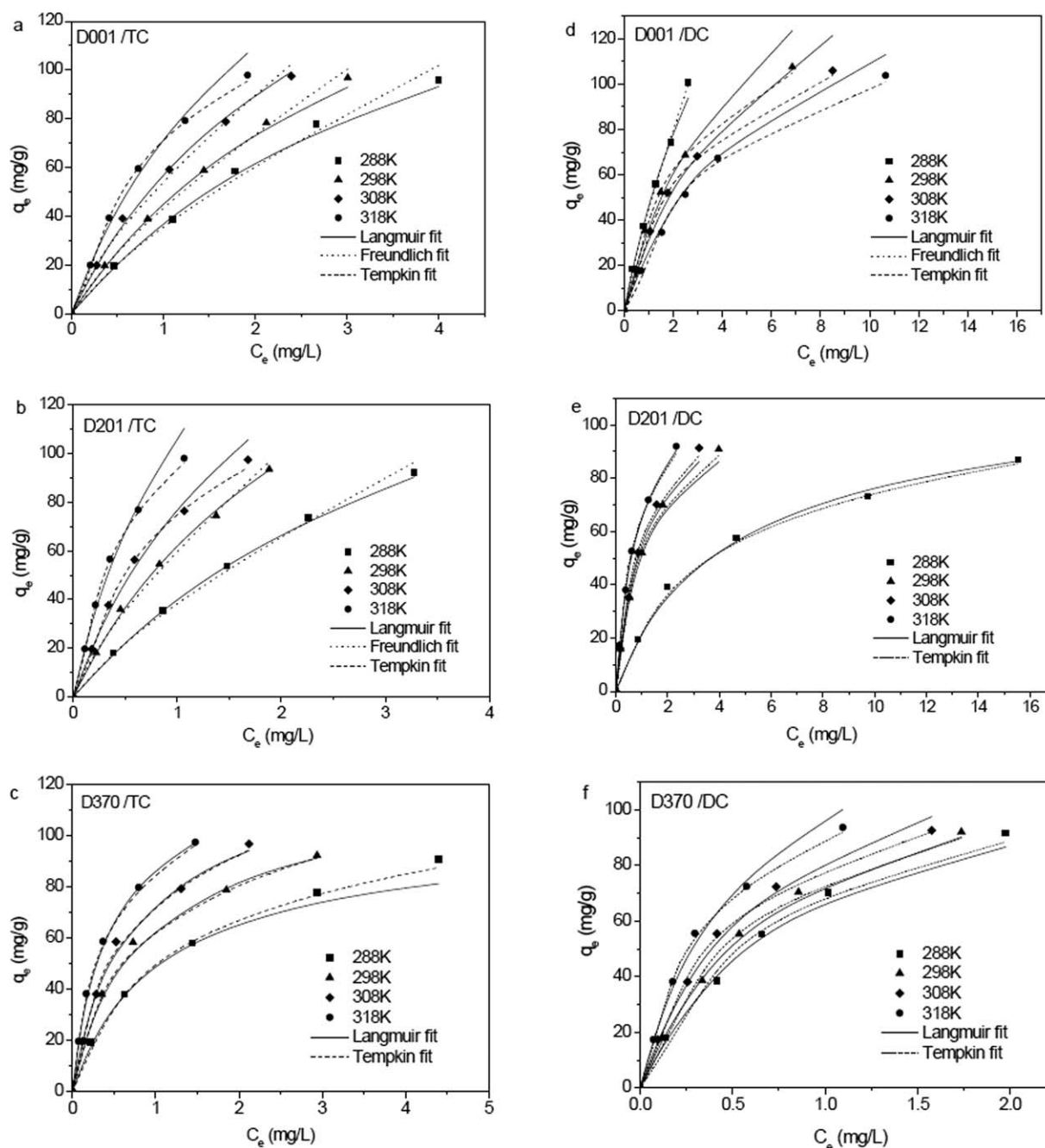


Figure 5. Adsorption isotherms for the adsorption of TC and DC onto resins D001, D201, and D370.

other hand, TC and DC mainly existed as cations at  $\text{pH} < 4$  and as anions at  $\text{pH} > 7$ . The four strong-acid resins exhibited good adsorption abilities at  $\text{pH} < 4$ ; this was mainly attributed to the electrostatic interaction between the negatively charged strong-acid resins and the positively charged TC or DC at low pH. Meanwhile, the stronger sorption capabilities of the basic resins D201 and D370 for TC and DC at high pH compared to that at low pH also supported this electrostatic interaction mechanism.

Furthermore, strong  $\pi$ - $\pi$  EDA interactions were verified between the TC molecule and the polarized polycyclic aromatic rings on the surface of carbonaceous adsorbents.<sup>18</sup> Both TC and

DC had a basic structure of four aromatic rings, and the adsorbents of the polystyrene resins also possessed polarized aromatic structures. So we proposed that the  $\pi$ - $\pi$  EDA interactions between the aromatic compound TC or DC ( $\pi$ -electron acceptor) and the  $\pi$  electron-rich regions on the surface of the resins also played an important role in the adsorption.

#### Effect of the Amounts of the Adsorbents

To investigate the optimal amounts of the resins, 10, 25, 50, 75, and 100 mg of D201 or D370 were introduced into the flasks containing 50 mL of 100 mg/L TC or DC solution ( $\text{pH} 7.0$ ). The measured results are depicted in Figure 3. The results demonstrate

**Table II.** Thermodynamic Parameters for the Adsorption of TC and DC onto Resins D001, D201, and D370

Drug	pH	Resin	$\Delta S^\circ$ (kJ·mol <sup>-1</sup> ·K <sup>-1</sup> )	$\Delta H^\circ$ (kJ/mol)	$\Delta G^\circ$ (kJ/mol)			
					288 K	298 K	308 K	318 K
TC	3	D001	0.11	22.90	-8.97	-9.91	-11.08	-12.25
	7	D201	0.15	34.28	-9.22	-11.03	-12.21	-13.87
	7	D370	0.13	28.24	-10.34	-11.85	-12.91	-14.46
DC	3	D001	-0.03	-18.59	-9.50	-9.21	-9.04	-8.49
	7	D201	0.17	39.59	-7.31	-10.70	-11.37	-12.59
	7	D370	0.11	21.56	-11.09	-11.98	-13.17	-14.48

that the Ads.% value of TC and DC increased sharply with increasing amount of adsorbents from 10 to 50 mg. Then, the Ads.% increased slowly and remained almost constant when the adsorbent dose increased further to 100 mg. The Ads.% values were all above 90% when the amount of adsorbents exceeded 50 mg. Herein, 50 mg have been the appropriate amount, and it was chosen in further studies for the removal of TC and DC.

#### Effect of the Ionic Strength

The effect of the ionic strength on the sorption capacities of TC and DC onto resins D201 and D370 was tested in 0–0.17 mol/L NaCl. From the results (Figure 4), we observed that the sorption depended on the ionic strength, and the sorption capacity decreased as the NaCl concentration increased. The sorption capacity decreased obviously with increasing NaCl from 0 to 0.02 mol/L; then, it decreased slowly and reached a plateau when the ionic strength of NaCl further increased to 0.17 mol/L. For resin D201, the inhibitory effect of the ionic strength for the sorption was more potent than that of resin D370, and the sorption capacities of TC and DC decreased by 72.9 and 67.3%, respectively, when the concentration of NaCl was 0.17 mol/L in the solution. However, for resin D370, the sorption capacities of TC and DC only decreased by 37.5 and 18.6%, respectively, at the same certain ionic concentration. This phenomenon was probably due to the competition between the antibiotic and electrolyte for the ion-exchange groups on the resins.

#### Adsorption Isotherms

We studied the equilibrium isotherms at various temperatures by varying the initial concentration of TC and DC under pH 3.0 for resin D001 and pH 7.0 for resins D201 and D370. The change in the adsorption capacities with equilibrium concentrations are given in Figure 5. An obviously greater sorption was observed as the temperature increased from 288 to 318 K, except in DC sorption onto D001; this indicated that DC sorption onto D001 was exothermic, whereas all of the other sorption processes were endothermic.<sup>31</sup>

Analysis of the isotherm data is of crucial importance in the design of the adsorption system. In this study, three common isotherm models, the Langmuir, Freundlich, and Tempkin isotherm models, were used to fit to the equilibrium data for TC and DC adsorption onto resins D001, D201, and D370. The linear mathematical forms of these isotherm models are summarized in Table S2 in the Supporting Information. The ideal Langmuir model reflects a uniform adsorbent surface and mono-

layer adsorption on specific homogeneous sites.<sup>34</sup> The empirical Freundlich model represents multilayer adsorption on heterogeneous surfaces.<sup>35</sup> The Tempkin model is a proper model for chemical adsorption based on strong electrostatic interaction between positive and negative charges.<sup>36</sup> The parameters of these isotherm models along with  $R^2$  values are summarized in the Supporting Information (Table S4). The two isotherm equations fitting the experimental data best for TC and DC sorption onto the resins are shown in Figure 5. The fitted results showed that the isotherm equations correlated the data with  $R^2$  values in the order Langmuir > Tempkin ~ Freundlich. Langmuir was the best equation for describing the experiment data for the sorption of TC and DC with the highest  $R^2$  (0.9909–0.9999). The Langmuir maximum adsorption capacities were 192.3, 204.1, and 113.6 mg/g for TC and 208.3, 109.9, and 128.2 mg/g for DC onto D001 (pH 3.0), D201, and D370 (pH 7.0), respectively, at 298 K, as an example. The dimensionless separation factor values were always lower than 1 and greater than 0 for all of the adsorbents; this indicated a favorable behavior toward TC and DC sorption at the studied concentrations.<sup>37</sup> The values of Freundlich constant  $1/n$  calculated by the Freundlich equation were always less than 1 (0.495–0.835) at all temperatures; this also indicated that the adsorption was favorable. Except for the sorption of TC onto D001 and D370 and the sorption of DC onto D001 at low temperature, the Tempkin model provided a slightly better fit to the observed data than the Freundlich model. This good fit given by Tempkin illustrated that there was electrostatic interaction in the process of adsorption.<sup>36</sup>

#### Thermodynamic Studies

The feature of the sorption process can be illustrated by thermodynamics analysis from the aspect of energy change. The thermodynamics parameters for the TC and DC sorption onto resins D001, D201, and D370 were evaluated by the experimental data under different temperatures, as shown in Figure 5. The thermodynamic parameters, including the Gibbs free energy ( $\Delta G^\circ$ ), enthalpy ( $\Delta H^\circ$ ), and entropy ( $\Delta S^\circ$ ), were calculated by the following equations and are tabulated in Table II:

$$\ln K_d = \frac{\Delta S^\circ}{R} - \frac{\Delta H^\circ}{RT} \quad (3)$$

$$\Delta G^\circ = -RT \ln K_d \quad (4)$$

where  $K_d$  is the distribution coefficient, which is the ratio of the amount adsorbed on the solid to the residual concentration in

solution at equilibrium,  $T$  is the temperature (K), and  $R$  is the universal gas constant ( $8.314 \text{ J}\cdot\text{mol}^{-1}\cdot\text{K}^{-1}$ ). The  $\Delta G^\circ$  values were found to be negative at all temperatures, showing that the sorption of TC and DC onto resins under certain pH conditions was thermodynamically feasible and spontaneous. For most adsorption processes, except DC sorption onto D001, the absolute  $\Delta G^\circ$  values increased with increasing temperature; this indicated an increase in the feasibility of these adsorptions at higher temperatures. The values of  $\Delta S^\circ$  were all positive for these adsorptions, and this demonstrated an increase in randomness at the adsorbate–solution interface during the sorption process.<sup>36</sup> The obtained  $\Delta H^\circ$  values were 22.9, 34.3, and 28.2 kJ/mol for TC sorption and  $-18.6$ , 39.6, and 21.6 kJ/mol for DC sorption onto D001, D201, and D370, respectively. These results indicate the exothermic features of DC sorption onto D001 but an endothermic nature for all of the other sorption processes. The magnitude of  $\Delta H^\circ$  gave indication on the type of sorption, which could be either physical or chemical sorption. If the absolute  $\Delta H^\circ$  was in the range 2.1–20.9 kJ/mol, the sorption process was supposed to proceed via physisorption.<sup>38</sup> According to the values of  $\Delta H^\circ$  obtained in this study, only the sorption of DC onto D001 at pH 3 took place via physical sorption.

## CONCLUSIONS

From the results of TC and DC sorption onto the six resins, the main conclusions were drawn as follows:

1. The pseudo-second-order kinetics model fit the data best for DC sorption onto the six resins and TC sorption onto D201 and D370, but the pseudo-first-order model fit the data of TC sorption onto the four strong-acid resins better at pH 7.0. Sorption equilibrium was reached after about 96 h.
2. The sorption exhibited strong pH dependence. For the basic resins D201 and D370, the best sorption pH conditions ranged from 4 to 7 for TC and were at pH 7 for DC. However, the good pH for TC and DC sorption onto the strong-acid resins was pH 2–3.
3. The Langmuir isotherm model provided the best match for the equilibrium adsorption data, with the sorption maxima reaching 192.31, 204.08, and 113.64 mg/g for TC and 208.33, 109.89, and 128.21 mg/g for DC onto D001 (pH 3.0), D201, and D370 (pH 7.0), respectively, at 298 K.
4. The sorption of TC and DC onto the resins was thermodynamically feasible and spontaneous, and the sorption process was endothermic, except for DC sorption onto D001 at pH 3.0.
5. The selected resins demonstrated excellent potential abilities in the removal of two common TCs (TC and DC) under certain conditions. DC sorption onto D001 at pH 3.0 was a physical process, and the other sorption processes have been dominated by chemisorptions. Electrostatic interactions, hydrophobic effects, and  $\pi$ – $\pi$  EDA interactions were important factors influencing the sorption process.

## ACKNOWLEDGMENTS

This work was financially supported by the National Nature Science Foundation of China (contract grant numbers 21376111,

21276117, and 21166009), the Natural Science Foundation of Jiangsu Province (contract grant numbers BK2011506 and BK2012697), and the Doctoral Innovation Fund of Jiangsu of Jiangsu Province (contract grant number CXLX12\_0667).

## REFERENCES

1. Michael, I.; Rizzo, L.; McArdell, C. S.; Manaia, C. M.; Merlin, C.; Schwartz, T.; Dagot, C.; Fatta-Kassinos, D. *Water Res.* **2013**, *47*, 957.
2. Andersson, D. I. *Curr. Opin. Microbiol.* **2003**, *6*, 452.
3. Kummerer, K. *Chemosphere* **2009**, *75*, 435.
4. Dirany, A.; Sires, I.; Oturan, N.; Ozcan, A.; Oturan, M. A. *Environ. Sci. Technol.* **2012**, *46*, 4074.
5. Kovalova, L.; Siegrist, H.; Singer, H.; Wittmer, A.; McArdell, C. S. *Environ. Sci. Technol.* **2012**, *46*, 1536.
6. Bajpai, S. K.; Bhowmik, M. *J. Appl. Polym. Sci.* **2010**, *117*, 3615.
7. Singh, T.; Singhal, R. *J. Appl. Polym. Sci.* **2013**, *129*, 3126.
8. Haham, H.; Oren, A.; Chefetz, B. *Environ. Sci. Technol.* **2012**, *46*, 11870.
9. Wang, Y. J.; Jia, D. A.; Sun, R. J.; Zhu, H. W.; Zhu, D. M. *Environ. Sci. Technol.* **2008**, *42*, 3254.
10. Kang, J.; Liu, H. J.; Zheng, Y. M.; Qu, J. H.; Chen, J. P. *J. Colloid Interface Sci.* **2011**, *354*, 261.
11. Chang, P. H.; Li, Z. H.; Yu, T. L.; Munkhbayer, S.; Kuo, T. H.; Hung, Y. C.; Jean, J. S.; Lin, K. H. *J. Hazard. Mater.* **2009**, *165*, 148.
12. Basakcilaran-Kabakci, S.; Thompson, A.; Cartmell, E.; Le Corre, K. *Water Environ. Res.* **2007**, *79*, 2551.
13. Liu, H.; Liu, W. F.; Zhang, J.; Zhang, C. L.; Ren, L.; Li, Y. J. *Hazard. Mater.* **2011**, *185*, 1528.
14. Choi, K. J.; Kim, S. G.; Kim, S. H. *J. Hazard. Mater.* **2008**, *151*, 38.
15. Zhang, D.; Pan, B.; Zhang, H.; Ning, P.; Xing, B. S. *Environ. Sci. Technol.* **2010**, *44*, 3806.
16. Ji, L. L.; Chen, W.; Zheng, S. R.; Xu, Z. Y.; Zhu, D. Q. *Langmuir* **2009**, *25*, 11608.
17. Cho, H. H.; Huang, H.; Schwab, K. *Langmuir* **2011**, *27*, 12960.
18. Ji, L. L.; Chen, W.; Duan, L.; Zhu, D. Q. *Environ. Sci. Technol.* **2009**, *43*, 2322.
19. Gao, Y.; Li, Y.; Zhang, L.; Huang, H.; Hu, J. J.; Shah, S. M.; Su, X. G. *J. Colloid Interface Sci.* **2012**, *368*, 540.
20. Ji, L. L.; Wan, Y. Q.; Zheng, S. R.; Zhu, D. Q. *Environ. Sci. Technol.* **2011**, *45*, 5580.
21. Xu, L. C.; Dai, J. D.; Pan, J. M.; Li, X. X.; Huo, P. W.; Yan, Y. S.; Zou, X. B.; Zhang, R. X. *Chem. Eng. J.* **2011**, *174*, 221.
22. Gezer, N.; Gulfen, M.; Aydin, A. O. *J. Appl. Polym. Sci.* **2011**, *122*, 1134.
23. Lee, C.; Helmy, R.; Strulson, C.; Plewa, J.; Kolodziej, E.; Antonucci, V.; Mao, B.; Welch, C. J.; Ge, Z. H.; Al-Sayah, M. A. *Org. Process. Res. Dev.* **2010**, *14*, 1021.

24. Yang, W. B.; Lu, Y. P.; Zheng, F. F.; Xue, X. X.; Li, N.; Liu, D. M. *Chem. Eng. J.* **2012**, *179*, 112.
25. Vergili, I.; Barlas, H. *J. Sci. Ind. Res.* **2009**, *68*, 417.
26. Yang, W. B.; Zheng, F. F.; Xue, X. X.; Lu, Y. P. *J. Colloid Interface Sci.* **2011**, *362*, 503.
27. Yang, W. B.; Zheng, F. F.; Lu, Y. P.; Xue, X. X.; Li, N. *Ind. Eng. Chem. Res.* **2011**, *50*, 13892.
28. Zhou, Q.; Li, Z. Q.; Shuang, C. D.; Li, A. M.; Zhang, M. C.; Wang, M. Q. *Chem. Eng. J.* **2012**, *210*, 350.
29. Zhang, M. C.; Li, A. M.; Zhou, Q.; Shuang, C. D.; Zhou, W. W.; Wang, M. Q. *Micropor. Mesopor. Mater.* **2014**, *184*, 105.
30. Robberson, K. A.; Waghe, A. B.; Sabatini, D. A.; Butler, E. C. *Chemosphere* **2006**, *63*, 934.
31. Shi, S.; Fan, Y. W.; Huang, Y. M. *Ind. Eng. Chem. Res.* **2013**, *52*, 2604.
32. Ahmed, M. J.; Theydan, S. K. *Chem. Eng. J.* **2012**, *211*, 200.
33. Zhou, Q.; Zhang, M. C.; Shuang, C. D.; Li, Z. Q.; Li, A. M. *Chin. Chem. Lett.* **2012**, *23*, 745.
34. Parga, J. R.; Vazquez, V.; Gonzalez, G.; Cisneros, M. M. *Chem. Eng. Technol.* **2010**, *33*, 1582.
35. Ji, L. L.; Shao, Y.; Xu, Z. Y.; Zheng, S. R.; Zhu, D. Q. *Environ. Sci. Technol.* **2010**, *44*, 6429.
36. Tang, Y. L.; Guo, H. G.; Xiao, L.; Yu, S. L.; Gao, N. Y.; Wang, Y. L. *Colloid Surf. A* **2013**, *424*, 74.
37. Huang, L. H.; Sun, Y. Y.; Wang, W. L.; Yue, Q. Y.; Yang, T. *Chem. Eng. J.* **2011**, *171*, 1446.
38. Ahmed, M. J.; Theydan, S. K. *Chem. Eng. J.* **2013**, *214*, 310.